

Oppenheim, A.V. & Cuomo, K.M. "Chaotic Signals and Signal Processing"  
*Digital Signal Processing Handbook*  
Ed. Vijay K. Madisetti and Douglas B. Williams  
Boca Raton: CRC Press LLC, 1999

# 71

## Chaotic Signals and Signal Processing

---

Alan V. Oppenheim  
*Massachusetts Institute of Technology*

Kevin M. Cuomo  
*MIT  
Lincoln Laboratory*

- [71.1 Introduction](#)
- [71.2 Modeling and Representation of Chaotic Signals](#)
- [71.3 Estimation and Detection](#)
- [71.4 Use of Chaotic Signals in Communications](#)  
Self-Synchronization and Asymptotic Stability • Robustness and Signal Recovery in the Lorenz System • Circuit Implementation and Experiments
- [71.5 Synthesizing Self-Synchronizing Chaotic Systems](#)
- [References](#)

### 71.1 Introduction

---

Signals generated by chaotic systems represent a potentially rich class of signals both for detecting and characterizing physical phenomena and in synthesizing new classes of signals for communications, remote sensing, and a variety of other signal processing applications.

In classical signal processing a rich set of tools has evolved for processing signals that are deterministic and predictable such as transient and periodic signals, and for processing signals that are stochastic. Chaotic signals associated with the homogeneous response of certain nonlinear dynamical systems do not fall in either of these classes. While they are deterministic, they are not predictable in any practical sense in that even with the generating dynamics known, estimation of prior or future values from a segment of the signal or from the state at a given time is highly ill-conditioned. In many ways these signals appear to be noise-like and can, of course, be analyzed and processed using classical techniques for stochastic signals. However, they clearly have considerably more structure than can be inferred from and exploited by traditional stochastic modeling techniques.

The basic structure of chaotic signals and the mechanisms through which they are generated are described in a variety of introductory books, e.g., [1, 2] and summarized in [3].

Chaotic signals are of particular interest and importance in experimental physics because of the wide range of physical processes that apparently give rise to chaotic behavior. From the point of view of signal processing, the detection, analysis, and characterization of signals of this type present a significant challenge. In addition, chaotic systems provide a potentially rich mechanism for signal design and generation for a variety of communications and remote sensing applications.

## 71.2 Modeling and Representation of Chaotic Signals

---

The state evolution of chaotic dynamical systems is typically described in terms of the nonlinear state equation  $\dot{x}(t) = F[x(t)]$  in continuous time or  $x[n] = F(x[n-1])$  in discrete time. In a signal processing context, we assume that the observed chaotic signal is a nonlinear function of the state and would typically be a scalar time function. In discrete-time, for example, the observation equation would be  $y[n] = G(x[n])$ . Frequently the observation  $y[n]$  is also distorted by additive noise, multipath effects, fading, etc.

Modeling a chaotic signal can be phrased in terms of determining from clean or distorted observations, a suitable state space and mappings  $F(\cdot)$  and  $G(\cdot)$  that capture the aspects of interest in the observed signal  $y$ . The problem of determining from the observed signal a suitable state space in which to model the dynamics is referred to as the embedding problem. While there is, of course, no unique set of state variables for a system, some choices may be better suited than others. The most commonly used method for constructing a suitable state space for the chaotic signal is the method of delay coordinates in which a state vector is constructed from a vector of successive observations.

It is frequently convenient to view the problem of identifying the map associated with a given chaotic signal in terms of an interpolation problem. Specifically, from a suitably embedded chaotic signal it is possible to extract a codebook consisting of state vectors and the states to which they subsequently evolve after one iteration. This codebook then consists of samples of the function  $F$  spaced, in general, non-uniformly throughout state space. A variety of both parametric and nonparametric methods for interpolating the map between the sample points in state space have emerged in the literature, and the topic continues to be of significant research interest. In this section we briefly comment on several of the approaches currently used. These and others are discussed and compared in more detail in [4].

One approach is based on the use of locally linear approximations to  $F$  throughout the state space [5, 6]. This approach constitutes a generalization of autoregressive modeling and linear prediction and is easily extended to locally polynomial approximations of higher order. Another approach is based on fitting a global nonlinear function to the samples in state space [7].

A fundamentally rather different approach to the problem of modeling the dynamics of an embedded signal involves the use of hidden Markov models [8, 9, 10]. With this method, the state space is discretized into a large number of states, and a probabilistic mapping is used to characterize transitions between states with each iteration of the map. Furthermore, each state transition spawns a state-dependent random variable as the observation  $y[n]$ . This framework can be used to simultaneously model both the detailed characteristics of state evolution in the system and the noise inherent in the observed data. While algorithms based on this framework have proved useful in modeling chaotic signals, they can be expensive both in terms of computation and storage requirements due to the large number of discrete states required to adequately capture the dynamics.

While many of the above modeling methods exploit the existence of underlying nonlinear dynamics, they do not explicitly take into account some of the properties peculiar to *chaotic* nonlinear dynamical systems. For this reason, in principle, the algorithms may be useful in modeling a broader class of signals. On the other hand, when the signals of interest are truly chaotic, the special properties of chaotic nonlinear dynamical systems ought to be taken into account, and, in fact, may often be exploited to achieve improved performance. For instance, because the evolution of chaotic systems is acutely sensitive to initial conditions, it is often important that this numerical instability be reflected in the model for the system. One approach to capturing this sensitivity is to require that the reconstructed dynamics exhibit Lyapunov exponents consistent with what might be known about the true dynamics. The sensitivity of state evolution can also be captured using the hidden Markov model framework since the structural uncertainty in the dynamics can be represented in terms of the probabilistic state transactions. In any case, unless sensitivity of the dynamics is taken

into account during modeling, detection and estimation algorithms involving chaotic signals often lack robustness.

Another aspect of chaotic systems that can be exploited is that the long term evolution of such systems lies on an attractor whose dimension is not only typically non-integral, but occupies a small fraction of the entire state space. This has a number of important implications both in the modeling of chaotic signals and ultimately in addressing problems of estimation and detection involving these signals. For example, it implies that the nonlinear dynamics can be recovered in the vicinity of the attractor using comparatively less data than would be necessary if the dynamics were required everywhere in state space.

Identifying the attractor, its fractal dimension, and related invariant measures governing, for example, the probability of being in the neighborhood of a particular state on the attractor, are also important aspects of the modeling problem. Furthermore, we can often exploit various ergodicity and mixing properties of chaotic systems. These properties allow us to recover information about the attractor using a single realization of a chaotic signal, and assure us that different time intervals of the signal provide qualitatively similar information about the attractor.

### 71.3 Estimation and Detection

---

A variety of problems involving the estimation and detection of chaotic signals arises in potential application contexts. In some scenarios, the chaotic signal is a form of noise or other unwanted interference signal. In this case, we are often interested in detecting, characterizing, discriminating, and extracting known or partially known signals in backgrounds of chaotic noise. In other scenarios, it is the chaotic signal that is of direct interest and which is corrupted by other signals. In these cases we are interested in detecting, discriminating, and extracting known or partially known chaotic signals in backgrounds of other noises or in the presence of other kinds of distortion.

The channel through which either natural or synthesized signals are received can typically be expected to introduce a variety of distortions including additive noise, scattering, multipath effects, etc. There are, of course, classical approaches to signal recovery and characterization in the presence of such distortions for both transient and stochastic signals. When the desired signal in the channel is a chaotic signal, or when the distortion is caused by a chaotic signal, many of the classical techniques will not be effective and do not exploit the particular structure of chaotic signals.

The specific properties of chaotic signals exploited in detection and estimation algorithms depend heavily on the degree of *a priori* knowledge of the signals involved. For example, in distinguishing chaotic signals from other signals, the algorithms may exploit the functional form of the map, the Lyapunov exponents of the dynamics, and/or characteristics of the chaotic attractor such as its structure, shape, fractal dimension and/or invariant measures.

To recover chaotic signals in the presence of additive noise, some of the most effective noise reduction techniques proposed to date take advantage of the nonlinear dependence of the chaotic signal by constructing accurate models for the dynamics. Multipath and other types of convolutional distortion can best be described in terms of an augmented state space system. Convolution or filtering of chaotic signals can change many of the essential characteristics and parameters of chaotic signals. Effects of convolutional distortion and approaches to compensating for it are discussed in [11].

### 71.4 Use of Chaotic Signals in Communications

---

Chaotic systems provide a rich mechanism for signal design and generation, with potential applications to communications and signal processing. Because chaotic signals are typically broadband, noise-like, and difficult to predict, they can be used in various contexts in communications. A particularly useful class of chaotic systems are those that possess a self-synchronization property [12, 13, 14].

This property allows two identical chaotic systems to synchronize when the second system (receiver) is driven by the first (transmitter). The well-known Lorenz system is used below to further describe and illustrate the chaotic self-synchronization property.

The Lorenz equations, first introduced by E. N. Lorenz as a simplified model of fluid convection [15], are given by

$$\begin{aligned}\dot{x} &= \sigma(y - x) \\ \dot{y} &= rx - y - xz \\ \dot{z} &= xy - bz,\end{aligned}\tag{71.1}$$

where  $\sigma$ ,  $r$ , and  $b$  are positive parameters. In signal processing applications, it is typically of interest to adjust the time scale of the chaotic signals. This is accomplished in a straightforward way by establishing the convention that  $\dot{x}$ ,  $\dot{y}$ , and  $\dot{z}$  denote  $dx/d\tau$ ,  $dy/d\tau$ , and  $dz/d\tau$ , respectively, where  $\tau = t/T$  is normalized time and  $T$  is a time scale factor. It is also convenient to define the normalized frequency  $\omega = \Omega T$ , where  $\Omega$  denotes the angular frequency in units of rad/s. The parameter values  $T = 400 \mu\text{sec}$ ,  $\sigma = 16$ ,  $r = 45.6$ , and  $b = 4$  are used for the illustrations in this chapter.

Viewing the Lorenz system (71.1) as a set of transmitter equations, a dynamical receiver system that will synchronize to the transmitter is given by

$$\begin{aligned}\dot{x}_r &= \sigma(y_r - x_r) \\ \dot{y}_r &= rx(t) - y_r - x(t)z_r \\ \dot{z}_r &= x(t)y_r - bz_r.\end{aligned}\tag{71.2}$$

In this case, the chaotic signal  $x(t)$  from the transmitter is used as the driving input to the receiver system. In Section 71.4.1, an identified equivalence between self-synchronization and asymptotic stability is exploited to show that the synchronization of the transmitter and receiver is global, i.e., the receiver can be initialized in any state and the synchronization still occurs.

### 71.4.1 Self-Synchronization and Asymptotic Stability

A close relationship exists between the concepts of self-synchronization and asymptotic stability. Specifically, self-synchronization in the Lorenz system is a consequence of globally stable error dynamics. Assuming that the Lorenz transmitter and receiver parameters are identical, a set of equations that govern their error dynamics is given by

$$\begin{aligned}\dot{e}_x &= \sigma(e_y - e_x) \\ \dot{e}_y &= -e_y - x(t)e_z \\ \dot{e}_z &= x(t)e_y - be_z.\end{aligned}\tag{71.3}$$

where

$$\begin{aligned}e_x(t) &= x(t) - x_r(t) \\ e_y(t) &= y(t) - y_r(t) \\ e_z(t) &= z(t) - z_r(t).\end{aligned}$$

A sufficient condition for the error equations to be globally asymptotically stable at the origin can be determined by considering a Lyapunov function of the form

$$E(\mathbf{e}) = \frac{1}{2} \left( \frac{1}{\sigma} e_x^2 + e_y^2 + e_z^2 \right).$$

Since  $\sigma$  and  $b$  in the Lorenz equations are both assumed to be positive,  $E$  is positive definite and  $\dot{E}$  is negative definite. It then follows from Lyapunov's theorem that  $\mathbf{e}(t) \rightarrow 0$  as  $t \rightarrow \infty$ . Therefore,

synchronization occurs as  $t \rightarrow \infty$  regardless of the initial conditions imposed on the transmitter and receiver systems.

For practical applications, it is also important to investigate the sensitivity of the synchronization to perturbations of the chaotic drive signal. Numerical experiments are summarized in Section 71.4.2, which demonstrates the robustness and signal recovery properties of the Lorenz system.

### 71.4.2 Robustness and Signal Recovery in the Lorenz System

When a message or other perturbation is added to the chaotic drive signal, the receiver does not regenerate a perfect replica of the drive; there is always some synchronization error. By subtracting the regenerated drive signal from the received signal, successful message recovery would result if the synchronization error was small relative to the perturbation itself. An interesting property of the Lorenz system is that the synchronization error is *not* small compared to a narrowband perturbation; nevertheless, the message can be recovered because the synchronization error is nearly *coherent* with the message. This section summarizes experimental evidence for this effect; a more detailed explanation has been given in terms of an approximate analytical model [16].

The series of experiments that demonstrate the robustness of synchronization to white noise perturbations and the ability to recover speech perturbations focus on the synchronizing properties of the transmitter Eqs. (71.1) and the corresponding receiver equations,

$$\begin{aligned}\dot{x}_r &= \sigma(y_r - x_r) \\ \dot{y}_r &= rs(t) - y_r - s(t)z_r \\ \dot{z}_r &= s(t)y_r - bz_r.\end{aligned}\tag{71.4}$$

Previously, it was stated that with  $s(t)$  equal to the transmitter signal  $x(t)$ , the signals  $x_r$ ,  $y_r$ , and  $z_r$  will asymptotically synchronize to  $x$ ,  $y$ , and  $z$ , respectively. Below, we examine the synchronization error when a perturbation  $p(t)$  is added to  $x(t)$ , i.e., when  $s(t) = x(t) + p(t)$ .

First, we consider the case where the perturbation  $p(t)$  is Gaussian white noise. In Fig. 71.1, we show the perturbation and error spectra for each of the three state variables vs. normalized frequency  $\omega$ . Note that at relatively low frequencies, the error in reconstructing  $x(t)$  slightly exceeds the perturbation of the drive but that for normalized frequencies above 20 the situation quickly reverses. An analytical model closely predicts and explains this behavior [16]. These figures suggest that the sensitivity of synchronization depends on the spectral characteristics of the perturbation signal. For signals that are bandlimited to the frequency range  $0 < \omega < 10$ , we would expect that the synchronization errors will be larger than the perturbation itself. This turns out to be the case, although the next experiment suggests there are additional interesting characteristics as well.

In a second experiment,  $p(t)$  is a low-level speech signal (for example a message to be transmitted and recovered). The normalizing time parameter is  $400 \mu\text{sec}$  and the speech signal is bandlimited to 4 kHz or equivalently to a normalized frequency  $\omega$  of 10. Figure 71.2 shows the power spectrum of a representative speech signal and the chaotic signal  $x(t)$ . The overall chaos-to-perturbation ratio in this experiment is approximately 20 dB.

To recover the speech signal, the regenerated drive signal is subtracted at the receiver from the received signal. In this case, the recovered message is  $\hat{p}(t) = p(t) + e_x(t)$ . It would be expected that successful message recovery would result if  $e_x(t)$  was small relative to the perturbation signal. For the Lorenz system, however, although the synchronization error is not small compared to the perturbation, the message can be recovered because  $e_x(t)$  is nearly coherent with the message. This coherence has been confirmed experimentally and an explanation has been developed in terms of an approximate analytical model [16].

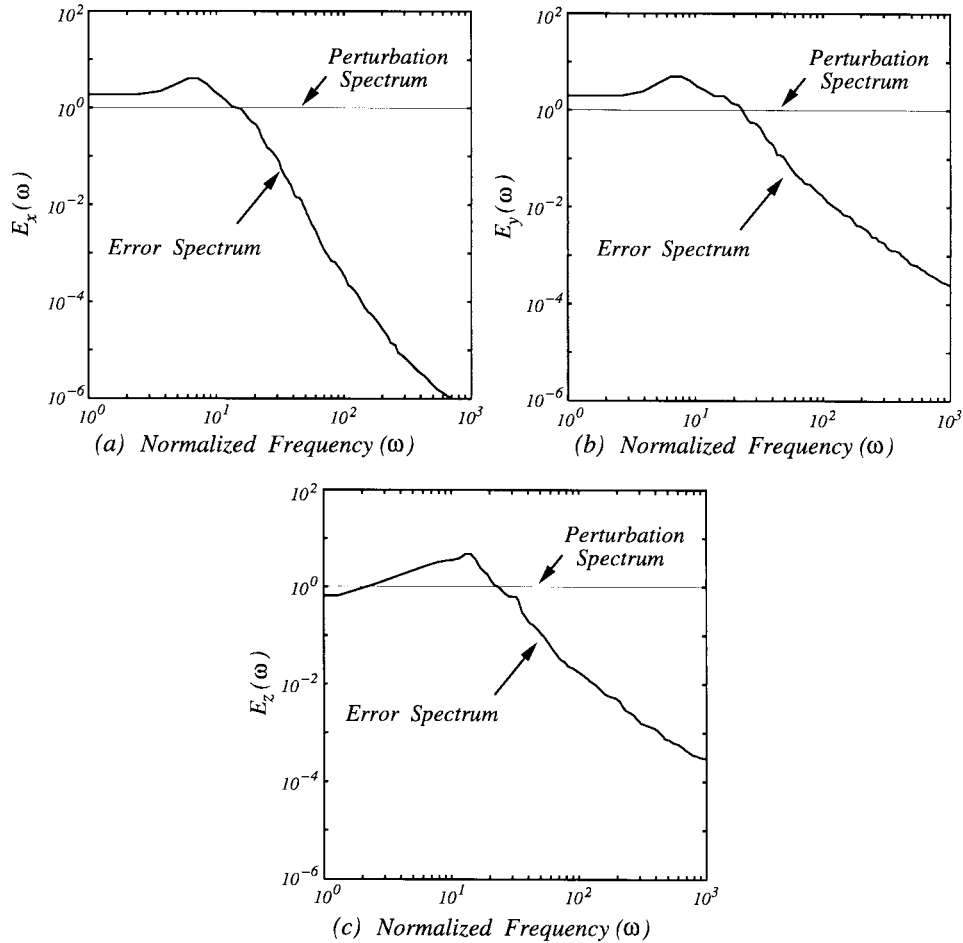


FIGURE 71.1: Power spectra of the error signals: (a)  $E_x(\omega)$ . (b)  $E_y(\omega)$ . (c)  $E_z(\omega)$ .

### 71.4.3 Circuit Implementation and Experiments

In Section 71.4.2, we showed that, theoretically, a low-level speech signal could be added to the synchronizing drive signal and approximately recovered at the receiver. These results were based on an analysis of the *exact* Lorenz transmitter and receiver equations. When implementing synchronized chaotic systems in hardware, the limitations of available circuit components result in approximations of the defining equations. The Lorenz transmitter and receiver equations can be implemented relatively easily with standard analog circuits [17, 20, 21]. The resulting system performance is in excellent agreement with numerical and theoretical predictions. Some potential implementation difficulties are avoided by scaling the Lorenz state variables according to  $u = x/10$ ,  $v = y/10$ , and  $w = z/20$ . With this scaling, the Lorenz equations are transformed to

$$\begin{aligned}\dot{u} &= \sigma(v - u) \\ \dot{v} &= ru - v - 20uw \\ \dot{w} &= 5uv - bw.\end{aligned}\tag{71.5}$$

For this system, which we refer to as the circuit equations, the state variables all have similar dynamic range and circuit voltages remain well within the range of typical power supply limits. Below, we

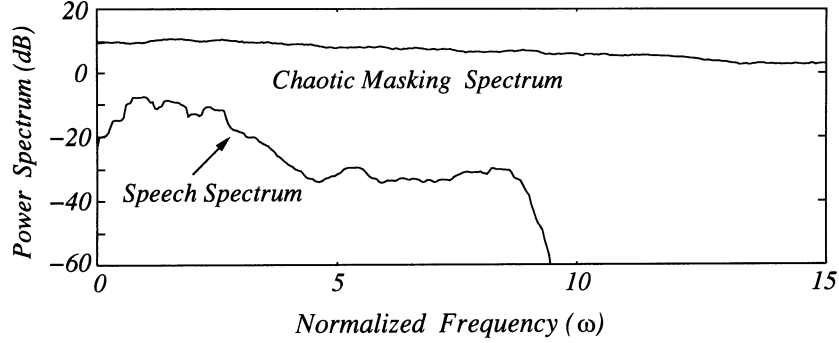


FIGURE 71.2: Power spectra of  $x(t)$  and  $p(t)$  when the perturbation is a speech signal.

discuss and demonstrate some applied aspects of the Lorenz circuits.

In Fig. 71.3, we illustrate a communication scenario that is based on chaotic signal masking and recovery [18, 19, 20, 21]. In this figure, a chaotic masking signal  $u(t)$  is added to the information-bearing signal  $p(t)$  at the transmitter, and at the receiver the masking is removed. By subtracting the regenerated drive signal  $u_r(t)$  from the received signal  $s(t)$  at the receiver, the recovered message is

$$\hat{p}(t) = s(t) - u_r(t) = p(t) + [u(t) - u_r(t)].$$

In this context,  $e_u(t)$ , the error between  $u(t)$  and  $u_r(t)$ , corresponds directly to the error in the recovered message.

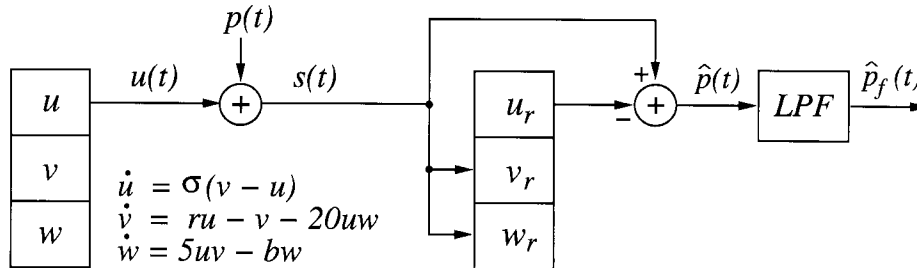


FIGURE 71.3: Chaotic signal masking and recovery system.

For this experiment,  $p(t)$  is a low-level speech signal (the message to be transmitted and recovered). The normalizing time parameter is  $400 \mu\text{sec}$  and the speech signal is bandlimited to 4 kHz or, equivalently, to a normalized frequency  $\omega$  of 10. In Fig. 71.4, we show the power spectrum of  $p(t)$  and  $\hat{p}(t)$ , where  $\hat{p}(t)$  is obtained from both a simulation and from the circuit. The two spectra for  $\hat{p}(t)$  are in excellent agreement, indicating that the circuit performs very well. Because  $\hat{p}(t)$  includes considerable energy beyond the bandwidth of the speech, the speech recovery can be improved by lowpass filtering  $\hat{p}(t)$ . We denote the lowpass filtered version of  $\hat{p}(t)$  by  $\hat{p}_f(t)$ . In Fig. 71.5(a) and (b), we show a comparison of  $\hat{p}_f(t)$  from both a simulation and from the circuit, respectively. Clearly, the circuit performs well and, in informal listening tests, the recovered message is of reasonable quality.

Although  $\hat{p}_f(t)$  is of reasonable quality in this experiment, the presence of additive channel noise will produce message recovery errors that cannot be completely removed by lowpass filtering; there



will always be some error in the recovered message. Because the message and noise are directly added to the synchronizing drive signal, the message-to-noise ratio should be large enough to allow a faithful recovery of the original message. This requires a communication channel that is nearly noise free.

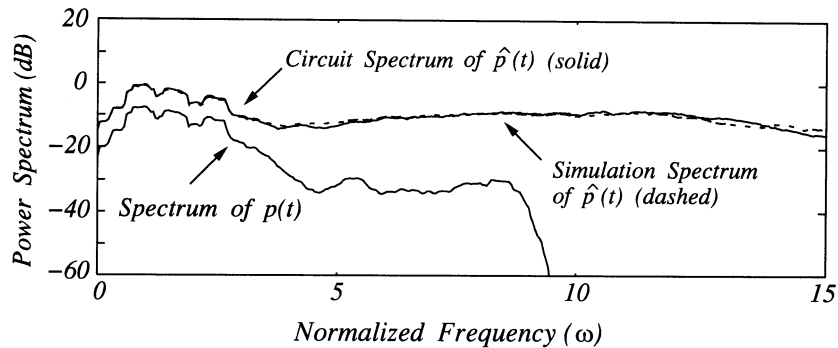


FIGURE 71.4: Power spectra of  $p(t)$  and  $\hat{p}(t)$  when the perturbation is a speech signal.

An alternative approach to private communications allows the information-bearing waveform to be exactly recovered at the self-synchronizing receiver(s), even when moderate-level channel noise is present. This approach is referred to as chaotic binary communications [20, 21]. The basic idea behind this technique is to modulate a transmitter parameter with the information-bearing waveform and to transmit the chaotic drive signal. At the receiver, the parameter modulation will produce a synchronization error between the received drive signal and the receiver's regenerated drive signal with an error signal amplitude that depends on the modulation. Using the synchronization error, the modulation can be detected.

This modulation/detection process is illustrated in Fig. 71.6. To illustrate the approach, we use a periodic square-wave for  $p(t)$  as shown in Fig. 71.7(a). The square-wave has a repetition frequency of approximately 110 Hz with zero volts representing the zero-bit and one volt representing the one-bit. The square-wave modulates the transmitter parameter  $b$  with the zero-bit and one-bit parameters given by  $b(0) = 4$  and  $b(1) = 4.4$ , respectively. The resulting drive signal  $u(t)$  is transmitted and the noisy received signal  $s(t)$  is used as the driving input to the synchronizing receiver circuit. In Fig. 71.7(b), we show the synchronization error power  $e^2(t)$ . The parameter modulation produces significant synchronization error during a "1" transmission and very little error during a "0" transmission. It is plausible that a detector based on the average synchronization error power, followed by a threshold device, could yield reliable performance. We illustrate in Fig. 71.7(c) that the square-wave modulation can be reliably recovered by lowpass filtering the synchronization error power waveform and applying a threshold test. The threshold device used in this experiment consisted of a simple analog comparator circuit.

The allowable data rate of this communication technique is, of course, dependent on the synchronization response time of the receiver system. Although we have used a low bit rate to demonstrate the technique, the circuit time scale can be easily adjusted to allow much faster bit rates.

While the results presented above appear encouraging, there are many communication scenarios where it is undesirable to be restricted to the Lorenz system, or for that matter, any other low-dimensional chaotic system. In private communications, for example, the ability to choose from a wide variety of synchronized chaotic systems would be highly advantageous. In the next section, we briefly describe an approach for synthesizing an unlimited number of high-dimensional chaotic systems. The significance of this work lies in the fact that the ability to synthesize high-dimensional

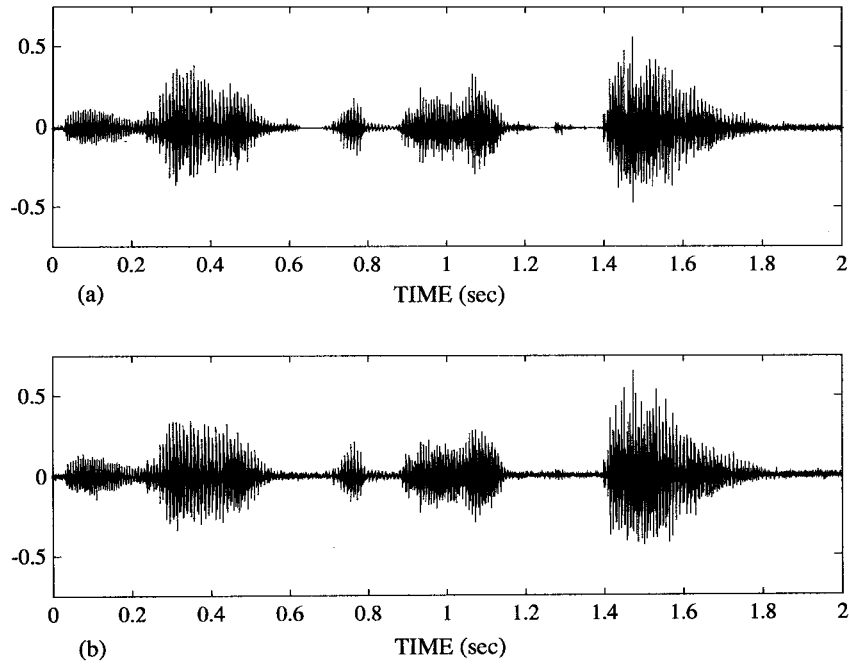


FIGURE 71.5: (a) Recovered speech (simulation). (b) Recovered speech (circuit).

chaotic systems further enhances their applicability for practical applications.

## 71.5 Synthesizing Self-Synchronizing Chaotic Systems

An effective approach to synthesis is based on a systematic four step process. First, an algebraic model is specified for the transmitter and receiver systems. As shown in [22, 23], the chaotic system models can be very general; in [22] the model represents a large class of quadratically nonlinear systems, while in [23] the model allows for an unlimited number of Lorenz oscillators to be mutually coupled via an  $N$ -dimensional linear system.

The second step in the synthesis process involves subtracting the receiver equations from the transmitter equations and imposing a global asymptotic stability constraint on the resulting error equations. Using Lyapunov's direct method, sufficient conditions for the error system's global sta-

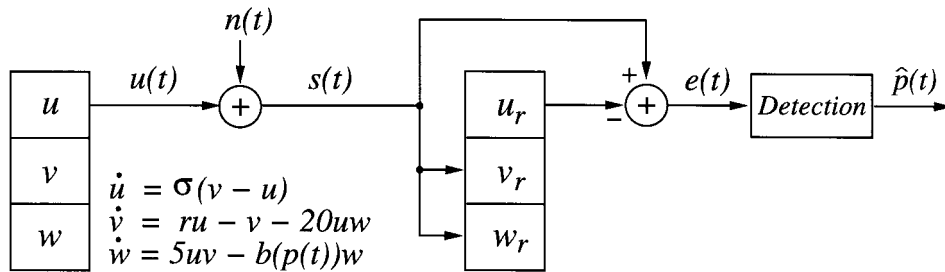


FIGURE 71.6: Communicating binary-valued bit streams with synchronized chaotic systems.

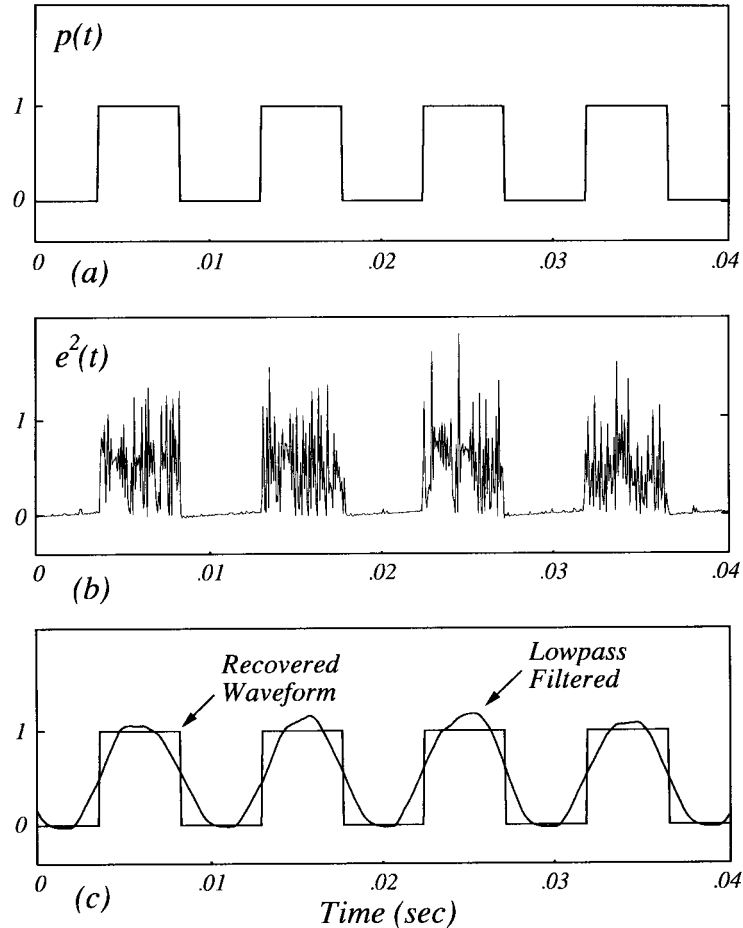


FIGURE 71.7: (a) Binary modulation waveform. (b) Synchronization error power. (c) Recovered binary waveform.

bility are usually straightforward to obtain. The sufficient conditions determine constraints on the free parameters of the transmitter and receiver which guarantee that they possess the global self-synchronization property.

The third step in the synthesis process focuses on the global stability of the transmitter equations. First, a family of ellipsoids in state space is defined and then sufficient conditions are determined which guarantee the existence of a *trapping region*. The trapping region imposes additional constraints on the free parameters of the transmitter and receiver equations.

The final step involves determining sufficient conditions that render all of the transmitter's fixed points unstable. In most cases, this involves numerically integrating the transmitter equations and computing the system's Lyapunov exponents and/or attractor dimension. If stable fixed points exist, the system's bifurcation parameter is adjusted until they all become unstable. Below, we demonstrate the synthesis approach for linear feedback chaotic systems.

Linear feedback chaotic systems (LFBCSs) are composed of a low-dimensional chaotic system and a linear feedback system as illustrated in Fig. 71.8. Because the linear system is  $N$ -dimensional,

considerable design flexibility is possible with LFBCSs. Another practical property of LFBCSs is that they synchronize via a single drive signal while exhibiting complex dynamics.

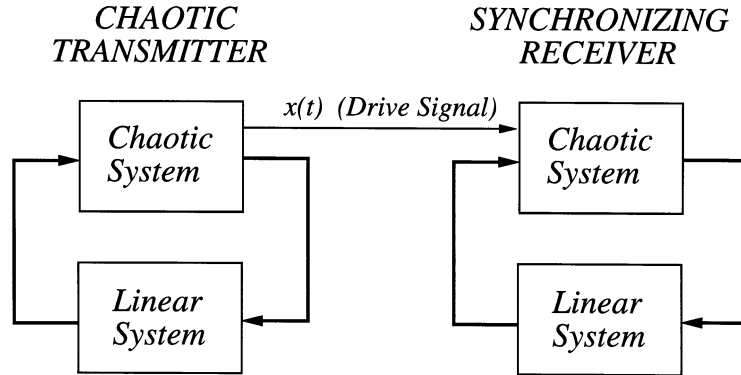


FIGURE 71.8: Linear feedback chaotic systems.

While many types of LFBCSs are possible, two specific cases have been considered in detail: (1) the chaotic Lorenz signal  $x(t)$  drives an  $N$ -dimensional linear system and the output of the linear system is added to the equation for  $\dot{x}$  in the Lorenz system; and (2) the Lorenz signal  $z(t)$  drives an  $N$ -dimensional linear system and the output of the linear system is added to the equation for  $\dot{z}$  in the Lorenz system. In both cases, a complete synthesis procedure was developed.

Below, we summarize the procedure; a complete development is given elsewhere [24].

### Synthesis Procedure

1. Choose any stable  $A$  matrix and any  $N \times N$  symmetric positive definite matrix  $Q$ .
2. Solve  $PA + A^T P + Q = 0$  for the positive definite solution  $P$ .
3. Choose any vector  $B$  and set  $C = -B^T P/r$ .
4. Choose any  $D$  such that  $\sigma - D > 0$ .

The first step of the procedure is simply the self-synchronization condition; it requires the linear system to be stable. Clearly, many choices for  $A$  are possible. The second and third steps are akin to a negative feedback constraint, i.e., the linear feedback tends to stabilize the chaotic system. The last step in the procedure restricts  $\sigma - D > 0$  so that the  $\dot{x}$  equation of the Lorenz system remains dissipative after feedback is applied.

For the purpose of demonstration, consider the following five-dimensional  $x$ -input/ $x$ -output LFBCS.

$$\begin{aligned}
 \dot{x} &= \sigma(y - x) + v \\
 \dot{y} &= rx - y - xz \\
 \dot{z} &= xy - bz
 \end{aligned}$$

$$\begin{bmatrix} \dot{l}_1 \\ \dot{l}_2 \end{bmatrix} = \begin{bmatrix} -\frac{1}{2} & 10 \\ -10 & -\frac{1}{2} \end{bmatrix} \begin{bmatrix} l_1 \\ l_2 \end{bmatrix} + \begin{bmatrix} 1 \\ 1 \end{bmatrix} x \tag{71.6}$$

$$v = - \begin{bmatrix} 1 & 1 \end{bmatrix} \begin{bmatrix} l_1 \\ l_2 \end{bmatrix}$$

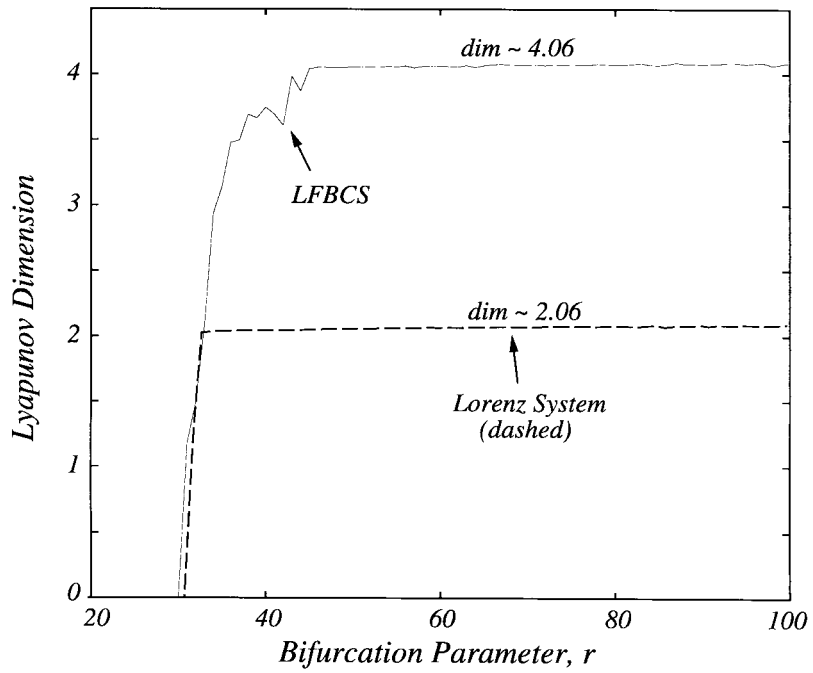


FIGURE 71.9: Lyapunov dimension of a 5-D LFBCS.

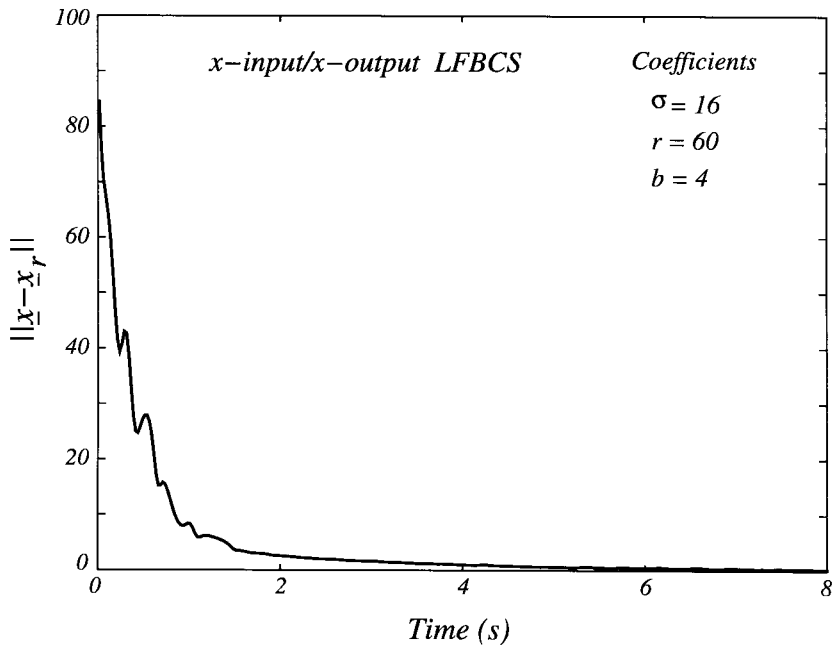


FIGURE 71.10: Self-synchronization in a 5-D LFBCS.

It can be shown in a straightforward way that the linear system satisfies the synthesis procedure for suitable choices of  $P$ ,  $Q$ , and  $R$ . For the numerical demonstrations presented below, the Lorenz parameters chosen are  $\sigma = 16$  and  $b = 4$ ; the bifurcation parameter  $r$  will be varied.

In Fig. 71.9, we show the computed Lyapunov dimension as  $r$  is varied over the range,  $20 < r < 100$ . This figure demonstrates that the LFBCS achieves a greater Lyapunov dimension than the Lorenz system without feedback. The Lyapunov dimension could be increased by using more states in the linear system. However, numerical experiments suggest that stable linear feedback creates only negative Lyapunov exponents, limiting the dynamical complexity of LFBCSs. Nevertheless, their relative ease of implementation is an attractive practical feature.

In Fig. 71.10, we demonstrate the rapid synchronization between the transmitter and receiver systems. The curve measures the distance in state space between the transmitter and receiver trajectories when the receiver is initialized from the zero state. Synchronization is maintained indefinitely.

## References

---

- [1] Moon, F., *Chaotic Vibrations*, John Wiley & Sons, New York, 1987.
- [2] Strogatz, S.H., *Nonlinear Dynamics and Chaos: with Applications to Physics, Biology, Chemistry, and Engineering*, Addison-Wesley, 1994.
- [3] Abarbanel, H.D.I., Chaotic signals and physical systems, *Proc. 1992 IEEE ICASSP*, IV, 113–116, 1992.
- [4] Sidorowich, J.J., Modeling of chaotic time series for prediction, interpolation and smoothing, *Proc. 1992 IEEE ICASSP*, IV, 121–124, 1992.
- [5] Singer, A., Oppenheim, A.V. and Wornell, G., Codebook prediction: A nonlinear signal modeling paradigm, *Proc. 1992 IEEE ICASSP*, V, 325–328, 1992.
- [6] Farmer, J.D. and Sidorowich, J.J., Predicting chaotic time series, *Phys. Rev. Lett.*, 59, 845, 1987.
- [7] Haykin, S. and Leung, H., Chaotic signal processing: First experimental radar results, *Proc. 1992 IEEE ICASSP*, IV, 125–128, 1992.
- [8] Meyers, C., Kay, S. and Richard, M., Signal separation for nonlinear dynamical systems, *Proc. 1992 IEEE ICASSP*, IV, 129–132, 1992.
- [9] Hsu, C.S., *Cell-to-Cell Mapping*, Springer-Verlag, 1987.
- [10] Meyers, C., Singer, A., Shin, B. and Church, E., Modeling chaotic systems with hidden Markov models, *Proc. 1992 IEEE ICASSP*, IV, 565–568, 1992.
- [11] Isabelle, S.H., Oppenheim, A.V. and Wornell, G.W., Effects of convolution on chaotic signals, *Proc. 1992 IEEE ICASSP*, IV, 133–136, 1992.
- [12] Pecora, L.M. and Carroll, T.L., Synchronization in chaotic systems, *Phys. Rev. Lett.*, 64(8), 821–824, Feb. 1990.
- [13] Pecora, L.M. and Carroll, T.L., Driving systems with chaotic signals, *Phys. Rev. A.*, 44, 2374–2383, Aug. 1991.
- [14] Carroll, T.L. and Pecora, L.M., Synchronizing chaotic circuits, *IEEE Trans. Circuits Syst.*, 38, 453–456, Apr. 1991.
- [15] Lorenz, E.N., Deterministic nonperiodic flow, *J. Atmospheric Sci.*, 20, 130–141, Mar. 1963.
- [16] Cuomo, K.M., Oppenheim, A.V. and Strogatz, S.H., Robustness and signal recovery in a synchronized chaotic system, *Int. J. Bifurcation Chaos*, 3(6), 1629–1638, Dec. 1993.
- [17] Cuomo, K.M. and Oppenheim, A.V., Synchronized chaotic circuits and systems for communications, *Technical Report 575*, MIT Research Laboratory of Electronics, 1992.
- [18] Cuomo, K.M., Oppenheim, A.V. and Isabelle, S.H., Spread spectrum modulation and signal masking using synchronized chaotic systems, *Technical Report 570*, MIT Research Laboratory of Electronics, 1992.

- [19] Oppenheim, A.V., Wornell, G.W., Isabelle, S.H. and Cuomo, K.M., Signal processing in the context of chaotic signals, in *Proc. 1992 IEEE ICASSP*, IV, 117–120, 1992.
- [20] Cuomo, K.M. and Oppenheim, A.V., Circuit implementation of synchronized chaos with applications to communications, *Phys. Rev. Lett.*, 71(1), 65–68, July 1993.
- [21] Cuomo, K.M., Oppenheim, A.V. and Strogatz, S.H., Synchronization of Lorenz-based chaotic circuits with applications to communications, *IEEE Trans. Circuits Syst*, 40(10), 626–633, Oct. 1993.
- [22] Cuomo, K.M., Synthesizing self-synchronizing chaotic systems, *Int. J. Bifurcation Chaos*, 3(5), 1327–1337, Oct. 1993.
- [23] Cuomo, K.M., Synthesizing self-synchronizing chaotic arrays, *Int. J. Bifurcation Chaos*, 4(3), 727–736, June 1994.
- [24] Cuomo, K.M., Analysis and synthesis of self-synchronizing chaotic systems, Ph.D. thesis, Massachusetts Institute of Technology, Feb. 1994.